

New results on soft particle production in heavy-ion collisions with ALICE

A. G. Knospe*

for the ALICE Collaboration

University of Houston

E-mail: anders.knospe@cern.ch

Studies of soft particle production play an important role in understanding the physics of heavy-ion collisions. Measurements of hadron yields are well described by grand-canonical thermal models in heavy-ion collisions, while an enhancement of strangeness production is observed in smaller collision systems. Several species of hadronic resonances are observed to be suppressed in central nucleus-nucleus collisions, likely due to scattering effects in the hadronic phase. The production mechanisms of nuclei can be studied through measurements of their yields, flow, and coalescence parameters. Hadron transverse-momentum spectra can be shaped by various effects, including radial flow and recombination; studies of the p_T spectra of identified hadrons with different masses and quark content can help to gauge the importance of such effects for different system sizes. Recent measurements by the ALICE Collaboration related to these topics will be presented for a wide range of system sizes in pp, p-Pb, Pb-Pb, and Xe-Xe collisions at LHC energies.

*Sixth Annual Conference on Large Hadron Collider Physics (LHCP2018)
4-9 June 2018
Bologna, Italy*

*Speaker.

The ALICE Collaboration at the LHC has conducted many measurements of soft particle production in ion-ion collisions. These proceedings present a selection of recent measurements of unidentified and identified hadron yields, hadronic resonances, nuclei, and the shapes of hadron p_T spectra. These results include new measurements in Xe–Xe collisions at $\sqrt{s_{NN}} = 5.44$ TeV and a precise measurement of the lifetime of the hypertriton.

ALICE has measured the charged-particle multiplicity $\langle dN_{ch}/d\eta \rangle$ at mid-rapidity in different multiplicity/centrality classes in pp, p–Pb, and A–A collisions at LHC energies [1]. This quantity does not scale with the number of participant nucleons $\langle N_{part} \rangle$: the ratio $2\langle dN_{ch}/d\eta \rangle/\langle N_{part} \rangle$ increases by about a factor of 2 from the most peripheral to the most central A–A collisions. However, an approximate scaling of $\langle dN_{ch}/d\eta \rangle$ is observed with $\langle N_{q-part} \rangle$, the number of wounded constituent quarks calculated using a quark-Glauber parameterization [2]. While measurements of $\langle dN_{ch}/d\eta \rangle$ in Xe–Xe and Pb–Pb collisions at similar energies are consistent for most values of $\langle N_{part} \rangle$, the 0–5% most central Xe–Xe collisions have a greater multiplicity than Pb–Pb collisions with similar $\langle N_{part} \rangle$. This behavior is not explained by $\langle N_{q-part} \rangle$ scaling and is not fully reproduced by model calculations. A hint of similar behavior may have been observed at RHIC [3] for Cu–Cu and Au–Au collisions (though with large uncertainties).

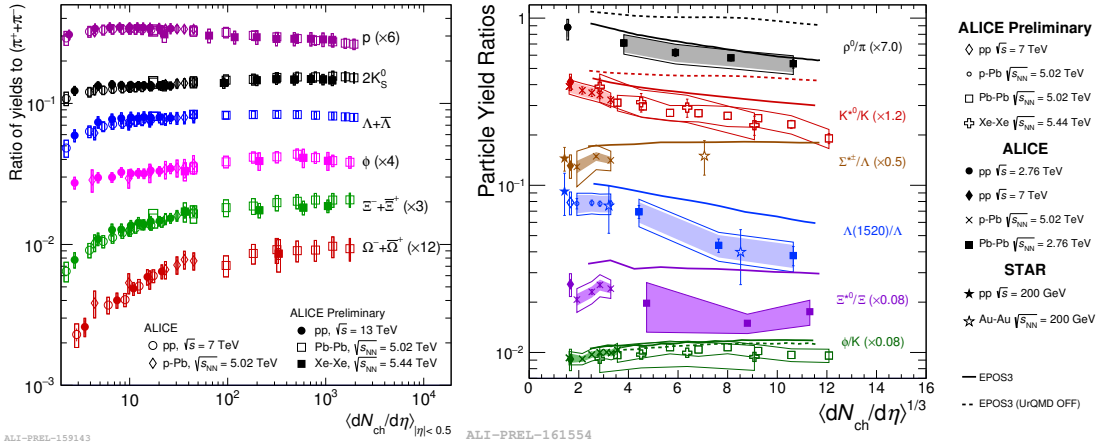


Figure 1: Left: Yield ratios of identified hadron to π^\pm as functions of $\langle dN_{ch}/d\eta \rangle$. Right: Yield ratios of resonances to long-lived hadrons [4, 5, 6] as functions of $\langle dN_{ch}/d\eta \rangle^{1/3}$ with values from the EPOS model [7].

The yields of most species of light-flavor hadrons in central Pb–Pb collisions are described with fair accuracy by grand-canonical thermal models [8]. Fits to ALICE measurements give chemical freeze-out temperatures of 153–156 MeV for Pb–Pb collisions at LHC energies. It is interesting to note that even the yield of nuclei and hyper-nuclei are well described by such calculations, despite the fact that their binding energies are much lower than the chemical freeze-out temperatures extracted from the models. There is, however, some tension between the models and the measurements for protons and strange baryons. This suggests the need for models that include additional effects, such as baryon annihilation, interactions in the hadron gas, or feed-down of excited hadronic states, as well as a better understanding of the impact of the quark composition on the hadronization process.

Fig. 1 (left) shows the yields of particles with 0 to 3 units of open strangeness (normalized to π yields) as a function of $\langle dN_{ch}/d\eta \rangle$ for many different collision systems at LHC energies. These

ratios evolve smoothly with $\langle dN_{\text{ch}}/d\eta \rangle$; for similar values of $\langle dN_{\text{ch}}/d\eta \rangle$, there is no dependence on the collision energy or the identity of the colliding nuclei. This suggests that hadron chemistry in the light-flavor sector is driven primarily by the multiplicity, which can be used as a proxy for the size of the collision system. These yield ratios saturate near the thermal-model values in large collision systems. There is an enhancement in strange-particle yields with multiplicity in small systems; particles with greater strangeness content exhibit a greater enhancement. As a “hidden strangeness” ($s\bar{s}$) state, the $\phi(1020)$ meson is a key probe for studying strangeness production. While particles with open strangeness are subject to canonical suppression in small systems, $\phi(1020)$ is not. The increase of the $\phi(1020)/\pi$ ratio in small systems is inconsistent with simple canonical suppression [9] and favors non-equilibrium production of $\phi(1020)$ or of all strange particles. The ratios $\phi(1020)/K$ and $\Xi/\phi(1020)$ are fairly flat across wide ranges of multiplicity, indicating that $\phi(1020)$ has an “effective strangeness” of 1-2 units.

While the yields of many light-flavor hadrons are viewed as being fixed at chemical freeze-out, the yields of short-lived resonances may be affected by scattering processes during the hadronic phase of heavy-ion collisions. Resonance yields may be regenerated through pseudo-elastic scattering of longer-lived hadrons. Resonances that decay during the hadronic phase may become un-reconstructable due to re-scattering of their decay products. The final resonance yields at kinetic freeze-out will depend on the chemical freeze-out temperature, the time between chemical and kinetic freeze out, the resonance lifetime, and the scattering cross sections of its decay products. Figure 1 (right) shows the yields of several resonances, normalized to the yields of long-lived hadrons with similar quark content. A multiplicity-dependent suppression of the $K^*(892)^0/K$, $\rho(770)^0/\pi$, and $\Lambda(1520)/\Lambda$ ratios is seen [4, 5, 6]. These three resonances have lifetimes ranging from 1.3 to 12.6 fm/c [10] and it appears that their yields have been reduced due to re-scattering in the hadronic phase. In contrast, the $\phi(1020)$ has a lifetime of 46.2 fm/c; it decays predominantly after the hadronic phase and is not strongly affected by re-scattering or regeneration. The $\Xi(1530)^0$ has a lifetime about half that of the $\phi(1020)$; the $\Xi(1530)^0/\Xi^-$ ratio exhibits possible weak suppression in central Pb–Pb collisions (in comparison to pp and p–Pb collisions). These ratios, too, seem to depend on the multiplicity $\langle dN_{\text{ch}}/d\eta \rangle$, but not on the collision energy (from RHIC to LHC energies) or the identity of the colliding nuclei. The ratios as functions of centrality in Pb–Pb collisions are described qualitatively by the EPOS model [7], which uses UrQMD [11] to describe hadronic scattering effects. Turning off UrQMD results in a poorer description of the $K^*(892)^0/K$ and $\rho(770)^0/\pi$ ratios.

The production of nuclei in large collision systems can be described using grand-canonical thermal models. Such models predict that yields of nuclei decrease with the nuclear mass, proportional to $e^{-m/T_{\text{ch}}}$, where m is the mass and T_{ch} is the chemical freeze-out temperature. In smaller systems, the production of nuclei can also be described using coalescence models, in which nuclei are formed by baryons that are close together in phase space at kinetic freeze out. Figure 2 (left) shows the d/p ratio for different collision systems as a function of $\langle dN_{\text{ch}}/d\eta \rangle$. The increase with multiplicity for small systems is consistent with production of deuterons through coalescence, while the flat behavior at high multiplicities is described by thermal models. As for other hadrons, deuteron production seems to evolve smoothly with the system size. The ${}^3\text{He}/p$ ratio is constant and described well by thermal models in A–A collisions, while an increasing trend is suggested for small systems. However, there is a factor of ≈ 5 increase in the ${}^3\text{He}/p$ ratio between p–Pb and Pb–

Pb collisions. It is unclear whether this is a true discontinuity (which would be difficult to explain) or if it is due to the coarse multiplicity/centrality binning of the measurement (which leaves a large multiplicity gap between the p–Pb and Pb–Pb measurements).

ALICE has also measured the flow of nuclei. Combined fits have been performed of the p_T spectra and v_2 values of π^\pm , K^\pm , and $p(\bar{p})$ using the blast-wave model [12]. The same set of parameters can be used to make predictions for nuclei. Basic coalescence models predict a simple relationship between v_2 values for protons and those for nuclei: for nucleus X with mass number A, $v_2^X(p_T^X) = Av_2^p(Ap_T^p)$. The blast-wave predictions for the p_T spectra and v_2 values of deuterons agree well with ALICE measurements in mid-central Pb–Pb collisions, particularly for $2 < p_T < 5$ GeV/c. This suggests a common kinetic freeze out for deuterons and the lighter hadrons. In contrast, the deuteron v_2 values predicted for simple coalescence are larger than those measured in mid-central Pb–Pb collisions. For ${}^3\text{He}$ in Pb–Pb collisions at $\sqrt{s_{\text{NN}}} = 5.02$ TeV, blast-wave predictions tend to underestimate v_2 , while a coalescence prediction provides a decent description for the 0-20% and 40-60% centrality classes; more events are needed to distinguish between these scenarios.

Deuteron production via coalescence can also be tested by computing the coalescence parameter B_2 . This should be flat for simple coalescence, but ALICE measurements exhibit a clear increase with p_T for mid-central Pb–Pb collisions [12]. While simple coalescence does not describe deuteron measurements in mid-central Pb–Pb collisions at LHC energies, it has described measurements in lower energy A–A collisions, and $B_2(p_T)$ has been observed to become flatter for smaller collision systems. As shown in 2 (right), B_2 decreases with increasing $\langle dN_{\text{ch}}/d\eta \rangle$ and evolves smoothly from small to large systems. This reinforces the conclusion that deuteron production is controlled primarily by the system size.

Rarer nuclei such as ${}^4\text{He}$ and the hypertriton ${}^3_\Lambda\text{H}$ (and the corresponding anti-nuclei) have also been measured. The yields of these species are well described by thermal models and clear evidence is seen for the expected exponential decrease in nucleus yields with mass. The ${}^3_\Lambda\text{H}$ lifetime has also been measured with high precision. As shown in Fig. 3, the world average has been somewhat lower than the lifetime of the free Λ . The newest ALICE measurement is consistent with both the world average and the free Λ lifetime, while being greater than a recent STAR measurement [13] of the ${}^3_\Lambda\text{H}$ lifetime.

ALICE has measured the mean transverse momentum $\langle p_T \rangle$ of unidentified and identified hadrons in many collision systems. Measurements of charged-hadron $\langle p_T \rangle$ values for Pb–Pb collisions at $\sqrt{s_{\text{NN}}} = 5.02$ TeV and Xe–Xe collisions at $\sqrt{s_{\text{NN}}} = 5.44$ TeV are consistent for similar centrality percentiles and are well described by hydrodynamic calculations [14]. In central A–A collisions, mass ordering is observed for the $\langle p_T \rangle$ values of identified hadrons, as shown in Fig. 4 (left). In particular, the $\langle p_T \rangle$ values of proton and $\phi(1020)$ are consistent with each other; this is expected in a hydrodynamic framework, where the shapes of hadron p_T spectra are determined by particle masses. This mass ordering is, however, violated for peripheral A–A, p–Pb, and pp collisions: $\langle p_T \rangle$ values for $\phi(1020)$ and $K^*(892)^0$ often exceed those for protons and Λ . In small collision systems, $\phi(1020)$ has $\langle p_T \rangle$ values approaching those for Ξ^- , despite the $\sim 30\%$ mass difference between those particles. Further theoretical input is needed to determine whether this is a manifestation of different behavior for baryons and mesons, or whether the resonances ($K^*(892)^0$ and $\phi(1020)$) behave differently than longer lived particles.

Simultaneous blast-wave fits have been performed for π^\pm , K^\pm , and $p(\bar{p})$ in various collision

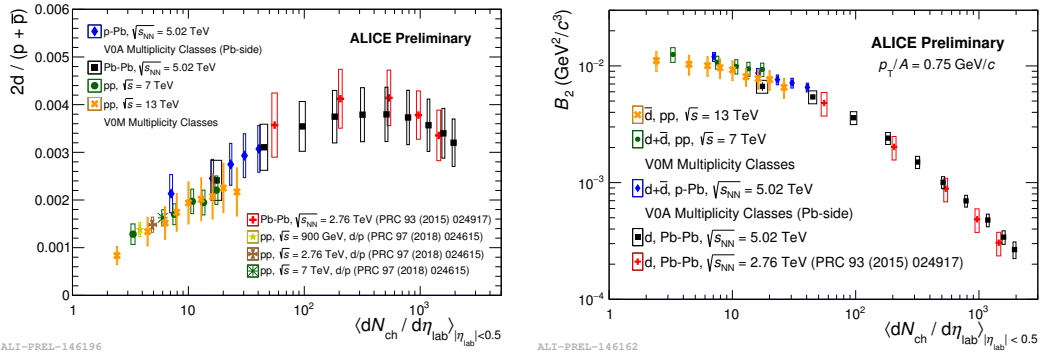
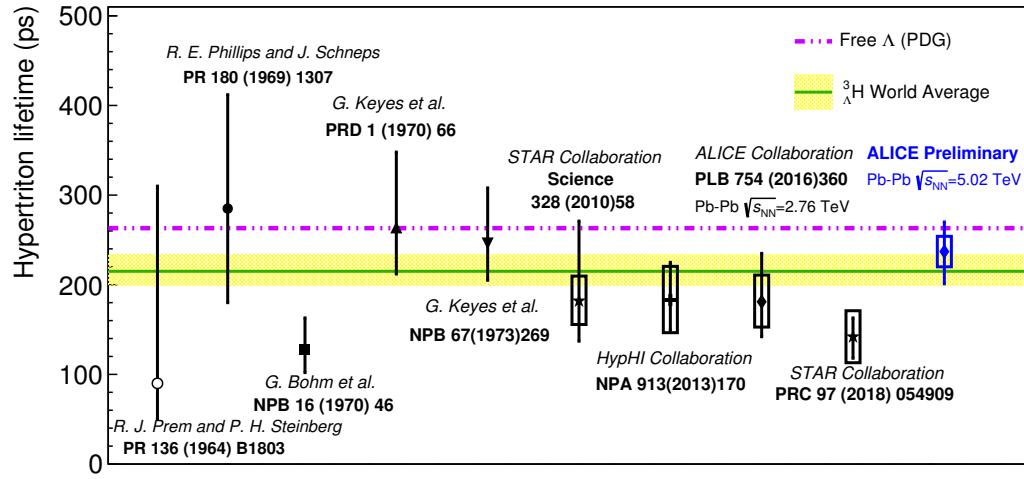


Figure 2: Left: Yield ratio of deuterons to protons as a function of $\langle dN_{ch}/d\eta \rangle$. Right: Deuteron coalescence parameter B_2 at $p_T/A = 0.75$ GeV/c as a function of $\langle dN_{ch}/d\eta \rangle$.



ALI-DER-161043

Figure 3: Summary of ${}^3\Lambda\text{H}$ lifetime measurements.

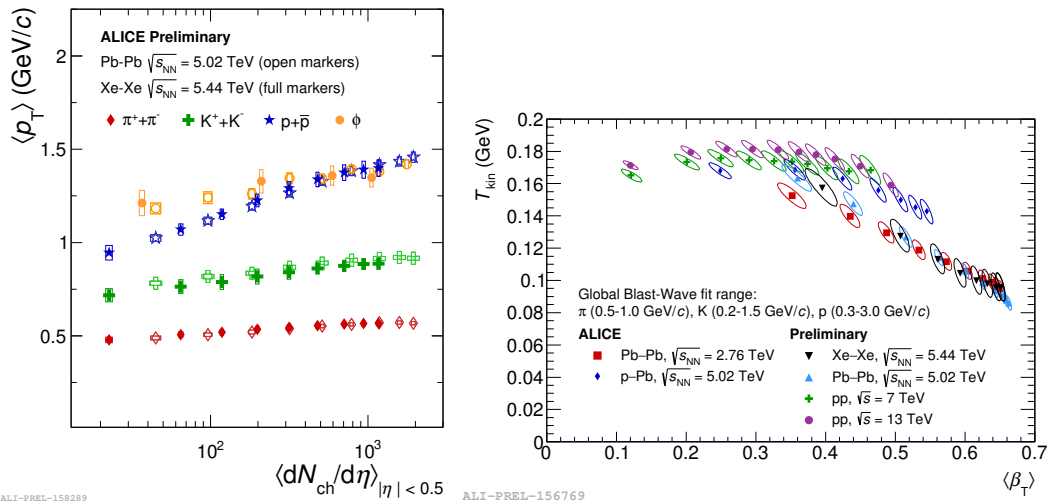


Figure 4: Left: Identified hadron $\langle p_T \rangle$ as a function of $\langle dN_{ch}/d\eta \rangle$ in A-A collisions. Right: Blast-wave fit parameters for various collision systems.

systems in multiplicity/centrality bins. As shown in Fig. 4 (right), the fit parameters for A–A collisions follow similar trends without any clear energy dependence: the kinetic freeze-out temperature decreases with increasing $\langle dN_{\text{ch}}/d\eta \rangle$, while the mean transverse flow velocity $\langle \beta_T \rangle$ increases. The fit parameters for p–Pb and pp collisions follow a trend that is distinct from the A–A trend: the kinetic freeze-out temperature does not depend strongly on multiplicity, while $\langle \beta_T \rangle$ increases rapidly with multiplicity.

The p_T -dependent ratios of baryon and meson yields can be used to study different mechanisms that determine the shapes of hadron p_T spectra. Enhancement of the Λ/K_S^0 and p/π ratios has been observed at intermediate p_T in central A–A collisions. In recombination models this can be explained as differences between the baryons and mesons. In a hydrodynamic interpretation, the increase from low to intermediate p_T can be viewed as a mass effect: both ratios involve a heavy baryon and a lighter meson. Studying the $p/\phi(1020)$ ratio, which involves a baryon and meson with similar masses, could help to disentangle mass and baryon-number effects. The $p/\phi(1020)$ ratio is observed to be constant with p_T for $p_T \lesssim 4$ GeV/ c in central A–A collisions (also seen in the $\langle p_T \rangle$ values) [4]. This is consistent with a simple hydrodynamic interpretation, but it should be emphasized that some recombination models [15] can also account for the constant behavior.

In summary, the measurements discussed above will allow for a better understanding of the physics of ion-ion collision systems of different sizes. Hadron yields evolve smoothly with $\langle dN_{\text{ch}}/d\eta \rangle$ from small to large collision systems, with short-lived resonances being suppressed due to re-scattering of their decay products in the hadronic phase. Simple coalescence models do not describe deuteron production in central A–A collisions well. In contrast to the yields, the shapes of hadron p_T spectra are not controlled just by the multiplicity, with small systems (pp and p–Pb) having harder p_T spectra than A–A collisions for similar values of $\langle dN_{\text{ch}}/d\eta \rangle$.

References

- [1] S. Acharya *et al.* (ALICE Collaboration), arXiv:1805.04432 (2018).
- [2] C. Loizides, *Phys. Rev. C* **94** (2016) 024914 [1603.07375].
- [3] B. Alver *et al.* (PHOBOS Collaboration), *Phys. Rev. C* **83** (2011) 024913 [1011.1940].
- [4] B. Abelev *et al.* (ALICE Collaboration), *Phys. Rev. C* **91** (2015) 024609 [1404.0495].
- [5] S. Acharya *et al.* (ALICE Collaboration), arXiv:1805.04365 (2018).
- [6] S. Acharya *et al.* (ALICE Collaboration), arXiv:1805.04361 (2018).
- [7] A. G. Knospe *et al.*, *Phys. Rev. C* **93** (2016) 014911 [1509.07895].
- [8] S. Acharya *et al.* (ALICE Collaboration), *Nucl. Phys. A* **971** (2018) 1-20 [1710.07531].
- [9] V. Vislavicius and A. Kalweit, arXiv:1610.03001 (2016).
- [10] M. Tanabashi *et al.* (Particle Data Group), *Phys. Rev. D* **98** (2018) 030001.
- [11] S. A. Bass *et al.*, *Prog. Part. Nucl. Phys.* **41** (1998) 255-369 [nucl-th/9803035].
- [12] S. Acharya *et al.*, *Eur. Phys. J. C* **77** (2017) 658 [1707.07304].
- [13] L. Adamczyk *et al.* (STAR Collaboration), *Phys. Rev. C* **97** (2018) 054909 [1710.00436].
- [14] S. Acharya *et al.* (ALICE Collaboration), arXiv:1805.04399 (2018).
- [15] V. Minissale *et al.*, *Phys. Rev. C* **92** (2015) 054904 [1502.06213].